Development of a Computational Framework for Multiphysics Multiphase Species Tracking using NEAMS Tools

INL/RPT-24-80404
Revision 0

Advanced Reactor Technologies

AUGUST 2024

Mauricio Tano,
Samuel Walker, and
Abdalla Abou-Jaoude

Idaho National Laboratory

Idaho National Laboratory

Battelle Energy Alliance manages INL for the U.S. Department of Energy's Office of Nuclear Energy

INL/RPT-24-80404
Revision 0

Development of a Computational Framework for Multiphysics Multiphase Species Tracking using NEAMS Tools

Mauricio Tano,
Samuel Walker, and
Abdalla Abou-Jaoude
Idaho National Laboratory

August 2024

Idaho National Laboratory
Advanced Reactor Technologies
Idaho Falls, Idaho 83415

http://www.art.inl.gov

Prepared for the
U.S. Department of Energy
Office of Nuclear Energy
Under DOE Idaho Operations Office
Contract DE-AC07-05ID14517

Page intentionally left blank

INL ART Program

Development of a Computational Framework for Multiphysics Multiphase Species Tracking using NEAMS Tools

INL/RPT-24-80404
Revision 0

August 2024

Technical Reviewer: (Confirmation of mathematical accuracy, and correctness of data and appropriateness of assumptions.)

08/19/2024

Rodrigo Gonzalez Gonzaga de Oliveira
Modeling & Simulation Professional

Date

Approved by:

08/20/2024

Michael E. Davenport
INL ART Project Manager

Date

8/29/2024

Michelle T. Sharp
INL Quality Assurance

Date

Page intentionally left blank

SUMMARY

This report implements a high-fidelity multiphysics modeling framework using the Nuclear Energy Advanced Modeling and Simulation program tools to track isotopic species in molten salt reactors (MSRs), with a specific focus on the 91-depletion chain within the MSR experiment (MSRE). The model integrates neutronics, thermal-hydraulics, depletion, and thermochemistry to simulate the production, transport, and phase transitions of isotopes under steady-state and transient conditions. The main findings reveal that isotopes, such as bromine-91, largely remain in the liquid phase, while others, including krypton-91and yttrium-91, transition to the gas phase, significantly influencing the reactor's radiological source term. The study also shows that during transients, like a reactivity insertion transient, rapid void formation, and the expansion of the liquid-gas interface led to substantial transfers of dissolved isotopes into the gas phase, altering isotope distribution and largely increasing the source term in the off-gas system. Additionally, the research highlights that short-lived isotopes dominate the initial off-gas response during transients, while longer-lived isotopes determine the equilibrium state, underscoring the necessity of dynamic simulations for accurate species tracking and reactor safety analysis. The developed methodology will be applied in the future to the tracking of a larger number of species and introduce other species tracking mechanisms such as deposition and plating.

Page intentionally left blank

ACKNOWLEDGMENTS

This manuscript was drafted on behalf of Idaho National Laboratory, operated by Battelle Energy Alliance, LLC, under contract no. DE-AC07-05ID14517 with the United States Department of Energy (DOE). This work was prepared for the United States Advanced Reactor Technologies for the Molten Salt Reactor Campaign. It made use of the resources of the High-Performance Computing Center at Idaho National Laboratory, which is supported by the Office of Nuclear Energy of the United States DOE and the Nuclear Science User Facilities under contract no. DE-AC07-05ID14517.

Page intentionally left blank

CONTENTS

FIGURES

Page intentionally left blank

ACRONYMS

MSR	Molten Salt Reactor
MSRE	Molten Salt Reactor Experiment
NEAMS	Nuclear Energy Advanced Modeling and Simulation program

Page intentionally left blank

Development of a Computational Framework for Multiphysics Multiphase Species Tracking using NEAMS Tools

1. INTRODUCTION

In the domain of molten salt reactor (MSR) design, the management and monitoring of isotopic species—particularly radionuclides—within the reactor system is of key importance [Walker et al. 2023]. Species tracking plays a crucial role in ensuring reactor safety, optimizing performance, and facilitating the long-term operation. It involves the identification, quantification, and spatial distribution analysis of various isotopes, including fission products, actinides, and other transmutation products within the reactor environment. The following sections describes the multifaceted importance of species tracking across key areas, such as containment, heat removal, reactivity, corrosion, and safeguards, which are key for the safe and efficient operation of MSRs.

One key need for species tracking is containment of radiological species [Worrall et al. 2018]. Containment within a nuclear reactor is fundamentally concerned with preventing the escape of radionuclides into the environment. Source term refers to the quantity and types of radioactive materials that could be released during normal operations or potential accidents. The accurate tracking of species within the reactor is critical to understanding the behavior of radionuclides, particularly under varying operational conditions. Species tracking provides insights into the movement and accumulation of radioactive isotopes within the reactor system, which is crucial for developing containment strategies and predicting potential releases.

The containment strategies in advanced reactors, such as MSRs, rely on an in-depth understanding of the behavior of fission products and other radionuclides in liquid and gaseous phases [Haubenreich and Engel 1970]. The mobility of these species within the reactor core, their interactions with coolant and structural materials, and their potential release pathways need to be accurately modeled to ensure effective containment. Furthermore, the source term analysis derived from species tracking informs the design of engineered safety features and the implementation of emergency response measures.

A second key need for species tracking is understanding heat removal in MSRs [Ho et al. 2013]. The removal of heat from the reactor core is another critical function where species tracking plays an essential role. In MSRs and other liquid-fueled reactors, the heat removal process is closely linked to the behavior of isotopic species within the coolant. As the coolant circulates through the reactor, isotopes may plate out on various surfaces, including heat exchangers, pipes, and structural components. The deposition of radioactive materials on these surfaces can impact the efficiency of heat transfer, leading to localized hot spots and potentially compromising the integrity of the cooling system.

Species tracking allows the monitoring of isotope deposition rates and locations within the reactor. By understanding where specific isotopes tend to accumulate, reactor operators can optimize the design and maintenance of the cooling system to prevent the buildup of radioactive deposits [Kovacic et al. 2018]. Additionally, species tracking data can be used to develop predictive models for isotopic behavior under different operational scenarios, enabling more effective management of the reactor's thermal-hydraulic conditions.

Additionally, species being extracted from the reactor core can significantly change the effective delayed neutron fraction, β_{eff}, which is important for the control of the reactor [Krepel et al. 2008]. Reactivity control is at the heart of nuclear reactor operation; the distribution of neutron precursors, such as delayed neutron emitters, is critical in determining the reactor's effective delayed neutron fraction β_{eff}. The β_{eff} is a key parameter that influences the reactor's response to changes in reactivity, and therefore, its safety and control.

Species tracking provides the necessary data to monitor and model the behavior of neutron precursors within the reactor. In liquid-fueled reactors, where fuel and fission products are not confined to fixed locations, the movement of these neutron precursors within the reactor core and coolant loop significantly affects the β_{eff}. Accurate species tracking enables the development of detailed reactivity feedback models that account for the spatial and temporal variations in precursor distribution. These models are needed for predicting the reactor's response to transient conditions such as changes in power demand or operational upsets. By understanding the movement and concentration of neutron precursors, operators can better manage reactivity and ensure the reactor remains within safe operating limits.

Species tracking is also important for corrosion predictions [Sridharan and Allen 2013]. Corrosion is a significant challenge in nuclear reactors, particularly in those using molten salts or other aggressive coolants. The interaction between fission products and structural materials can accelerate corrosion, potentially leading to the degradation of critical components and the breach of containment barriers.

Species tracking is vital for understanding the chemical interactions between fission products and reactor materials [Sandhi 2022]. By identifying which isotopes are most likely to contribute to corrosion and where they are likely to accumulate, reactor designers can select materials with greater resistance to corrosive effects. Additionally, species tracking data can inform the development of protective coatings or treatments that extend the life of structural components. In the context of MSRs, where the entire reactor system is exposed to high-temperature molten salts, the long-term integrity of the containment and structural materials is a major concern. Accurate tracking of corrosive species helps in predicting the lifespan of these materials and in implementing maintenance schedules that prevent catastrophic failures.

Finally, species tracking facilitates the design and implementation of advanced monitoring technologies, such as in-situ sensors and online analytical tools, which can provide real-time data on the distribution and concentration of fissile isotopes. These technologies enhance the ability to detect and respond to any anomalies that may indicate unauthorized diversion or misuse of nuclear materials.

There are multiple physical phenomena affecting the behavior of species in MSRs, as shown in Figure 1, which directly impact the distribution, transport, and fate of isotopic species. These phenomena include the deposition of insoluble particles on various interfaces, the generation of soluble particles due to corrosion, and the precipitation of particles due to redox reactions. Understanding these processes is critical for accurate species tracking and the overall safety and efficiency of MSRs.

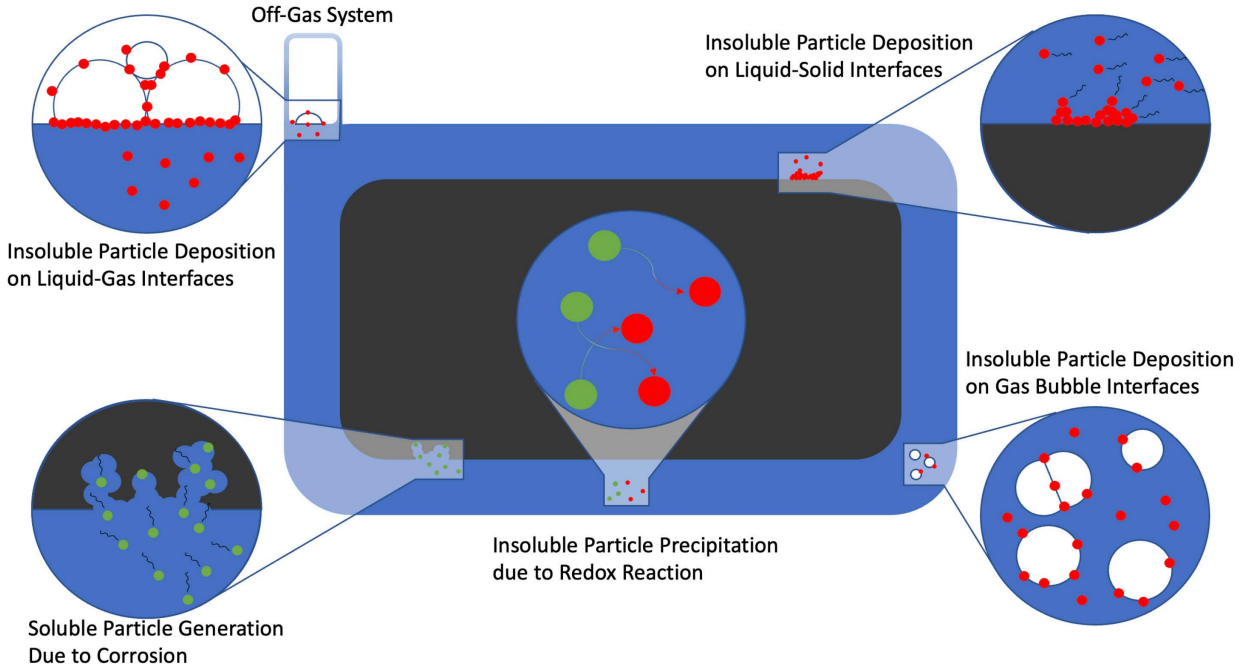

Figure 1. Key phenomena tacking place for species tracking in MSRs [Walker et al. 2023].

In MSRs, the interaction between liquid and gas phases plays a significant role in the deposition of insoluble particles inside the gas phases [Andrews et al. 2021]. These particles, which may consist of fission products, corrosion products, or other insoluble species, can accumulate at the liquid-gas interface due to differences in surface tension and buoyancy forces.

The process of generating species in the gas phase is influenced by several factors, including the chemical composition of the molten salt, the presence of surfactants or impurities, and the dynamics of gas bubble formation [Mcfarlane et al. 2020]. As gas bubbles rise through the molten salt, they can carry insoluble particles to the surface, where these particles may become trapped at the interface. This trapping effect is often enhanced by the surface-active nature of some species, which preferentially accumulate at the interface, forming a thin film or layer of particles. The accumulation of radioactive particles in the gas phase can lead to localized hot spots and may affect the overall heat transfer efficiency of the reactor. Moreover, if these particles are not removed, they can become a source term for airborne radioactive material, especially if they are released into the reactor's off-gas system.

Corrosion is an inherent challenge in MSRs due to the high-temperature, highly reactive environment of molten salts. As the reactor operates, the molten salt can corrode structural materials, leading to the release of soluble species into the salt. These soluble particles are typically metallic ions or chemical complexes that dissolve in the molten salt, altering its chemical composition and potentially affecting reactor performance. The generation of soluble particles due to corrosion is governed by electrochemical reactions at the interface between the molten salt and the reactor materials. The rate of corrosion and the types of soluble particles generated depend on factors such as the temperature, the composition of the salt, the presence of impurities, and the materials used in the reactor construction.

From a species tracking perspective, it is key to monitor the concentration and distribution of these soluble particles. Changes in the chemical composition of the molten salt can influence key reactor parameters, such as reactivity and heat transfer efficiency. Moreover, the buildup of soluble corrosion products can lead to secondary reactions, such as precipitation or deposition on other surfaces, further complicating the tracking of species within the reactor.

Insoluble particles generated within the molten salt can also deposit on solid-liquid interfaces, such as the surfaces of reactor components, pipes, and heat exchangers. This deposition process is driven by a combination of factors, including thermophoresis, sedimentation, and surface interactions. Thermophoresis, in particular, is a significant mechanism in MSRs, in which temperature gradients exist between the molten salt and the solid surfaces. Insoluble particles tend to migrate toward cooler regions, leading to their deposition on solid surfaces. This can result in the formation of scale or fouling layers, which can impact heat transfer efficiency and increase the risk of localized corrosion.

The interaction between insoluble particles and solid surfaces is also influenced by the chemical properties of the particles and the materials of the reactor components. For example, certain fission products may have a strong affinity for specific materials, leading to preferential deposition. This selective deposition can create regions of high radioactivity, posing challenges for reactor maintenance and decommissioning.

In the context of species tracking, understanding the patterns of insoluble particle deposition on solid-liquid interfaces is essential for predicting the long-term behavior of radioactive materials within the reactor. Accurate models of these processes can inform the design of reactor components to minimize deposition and facilitate the removal of deposited particles.

Insoluble particle deposition on gas bubble interfaces poses unique challenges for species tracking. The transient nature of gas bubbles and their interaction with particles complicate the prediction of particle transport and deposition patterns. Advanced computational models are required to accurately simulate these interactions and assess their impact on reactor safety and performance.

Redox reactions within the molten salt can lead to the precipitation of insoluble particles [Zhang et al. 2018]. These reactions are driven by changes in the oxidation state of species within the salt, which can occur due to interactions with reactor materials, fission products, or deliberate control measures (e.g., the addition of reductants or oxidants to control the chemistry of the salt).

Precipitation due to redox reactions is highly dependent on the local chemical environment within the reactor. For example, the reduction of certain metal ions can result in the formation of insoluble metallic particles, which then precipitate out of the molten salt. Similarly, the oxidation of specific species can lead to the formation of oxides or other insoluble compounds.

The formation and deposition of these precipitates are critical factors in species tracking, as they can alter the distribution of radioactive materials within the reactor. Precipitated particles may deposit on surfaces, agglomerate to form larger particles, or remain suspended in the molten salt, depending on their size and density. These behaviors must be accurately modeled to predict the long-term behavior of fission products and other radionuclides within the reactor.

This work will describe the advances for tracking species in MSRs in liquid and solid phases using the computational tools developed in the Nuclear Energy Advanced Modeling and Simulation (NEAMS) program. However, this is only a part of the framework needed for tracking species in MSRs. The rest of this work is organized as follows. In Section 2, the modeling framework for high-fidelity species tracking in MSRs is described including the modeling of neutron transport, depletion, two-phase thermal-hydraulics, and Eulerian species tracking in two phases. Then, in Section 3, this framework is applied for species tracking in the Molten Salt Reactor Experiment, while demonstrating both steady-state operation and a reactivity insertion transient.

2. MODELING FRAMEWORK

2.1. Neutronics Modeling for Species Tracking in Molten Salt Reactors

The transport of neutrons in the fuel loop of an MSR is described by the Boltzmann transport equation, which must be solved coupled with the circulating neutron precursors. In our model, the transport equation is simplified using the multi-group diffusion approximation, which is reasonable for the MSRs model due to the relatively homogeneous distribution in the reactor core and the high scattering cross sections when compared to the absorption ones. The three-dimensional neutronic solution of the neutron flux and precursor distribution in the reactor is carried out using Griffin, which is NEAMS's neutron transport and depletion modeling tool. Depletion is not integrated into our models owing to the low depletion expected for the MSR.

For steady state, the multi-group eigenvalue problem solved is Equation (1) [Gill and Azmy 2011]:

$$-\nabla \cdot D_g(\boldsymbol{r})\nabla \phi_g(\boldsymbol{r}) + \Sigma_{r,g}\, \phi_g(\boldsymbol{r}) = \frac{1-\beta_0}{k_{eff}}\, \chi_{p,g} \sum_{g'=1}^{G} \nu_{g'} \Sigma_{f,g'} \phi_{g'}(\boldsymbol{r}) + \sum_{g' \neq g}^{G} \Sigma_{s,g'} \phi_{g'}(\boldsymbol{r}) + \chi_{d,g} \sum_{i=1}^{m} \lambda_i c_i(\boldsymbol{r}) \quad (1)$$

where

D_g = Diffusion coefficient for energy group g

$\phi_g(\boldsymbol{r})$ = Neutron flux in energy group g at position $\boldsymbol{r}$

Σ_{rg} = Removal cross-section for energy group g

k_{eff} = Eigenvalue representing the effective multiplication factor of the reactor

$\chi_{p,g}$ = Prompt fission spectrum for energy group g

ν = Number of neutrons per fission at group g'

$\Sigma_{f,g'}$ = Fission cross-section for energy group g'

Σ'_{sg} = Differential scattering cross-section for energy group g' into energy group g

β_0 = Delayed neutrons fraction

$\chi_{d,g}$ = Delayed fission spectrum for energy group g

λ_i = Decay rate constant for precursor group i

$c_i(\boldsymbol{r})$ = Concentration of neutron precursor group at position } $\boldsymbol{r}$

G = Total number of energy groups.

The equation describes the neutron balance in a nuclear reactor with multiple energy groups, accounting for diffusion, scattering, fission, and removal processes. In the context of species tracking in MSR, the accurate modeling of neutron fluxes and precursor distributions is essential, as these quantities directly impact the production and transport of radioactive species. The neutron flux distribution governs the rate and location of fission reactions, thereby determining where fission products and other radionuclides are generated. Moreover, the transport of neutron precursors within the reactor core and fuel loop affects the delayed neutron fraction, which is critical for reactivity control and the dynamic behavior of the reactor.

The neutron precursors are modeled via an advection, diffusion, and reaction equation, which reads according to Equation (2) [Aufiero et al. 2014]:

$$\nabla \cdot \left(\boldsymbol{u}(\boldsymbol{r})c_i(\boldsymbol{r})\right) - \nabla \cdot H_i \nabla\, c_i(\boldsymbol{r}) - \nabla \cdot \frac{\nu_t}{Sc_t}\nabla c_i(\boldsymbol{r}) = \frac{\beta_0}{k_{eff}}\chi_{p,g}\ \sum_{g'=1}^{G}\nu_{g'}\Sigma_{f,g'}\phi_{g'}(\boldsymbol{r}) - \ \lambda_i c_i(\boldsymbol{r}) \quad (2)$$

The equation is solved simultaneously for the continuous circulating nuclear fuel.

where

$\boldsymbol{u}(\boldsymbol{r})$ = Advection velocity

H_i = Average molecular diffusion for neutron precursors of type i

ν_t = Turbulent kinematic viscosity

Sc_t = Turbulent Schmidt number.

The above system, defined by Equations (1)–(2), helps solve the neutron fluxes and precursor distribution in the reactor during steady state. The power and fission density can be directly computed from Equations (1)–(2). However, the spatial distribution of density and temperature fields are necessary to compute the spatial dependent nuclear cross sections. Additionally, the velocity field and turbulent kinematic viscosity are needed to compute the transport of neutron precursor groups. These fields are provided by a coupled thermal-hydraulics solution. Finally, the reactor will deform during operation due to thermal expansion. Due to the large amount of leakage in the MSR configuration, these deformations have a significant impact on reactivity. Hence, deformations must be computed with associated thermomechanics, which are solved and used in Griffin to update the solutions in the deforming mesh. The specific thermal-hydraulics and thermomechanics models used are described in detail in the next sections.

Species tracking in MSRs requires not only the steady-state solution but also an understanding of how the reactor responds to transient conditions. When evaluating a reactor transient, the impact of neutron precursors' advection into and out of the reactor core cannot be neglected as it will sensibly affect the reactor dynamics. Hence, for the transients solved, the steady-state eigenvalue problem is modified to add the neutron fluxes and precursor dynamics. The resulting equation set reads as follows in Equations (3)–(4):

$$\frac{1}{v_g}\frac{\partial \phi_g(\boldsymbol{r},t)}{\partial t} - \nabla \cdot\ D_g(\boldsymbol{r})\nabla\, \phi_g(\boldsymbol{r},t) + \Sigma_{r,g}\ \phi_g(\boldsymbol{r},t) = \frac{1-\beta_0}{k_{eff}^{st}}\ \chi_{p,g}\ \sum_{g'=1}^{G}\nu_{g'}\Sigma_{f,g'}\phi_{g'}(\boldsymbol{r},t) + \sum_{g'\neq g}^{G}\Sigma_{s,g'}\phi_{g'}(\boldsymbol{r},t)\ + \chi_{d,g}\sum_{i=1}^{m}\lambda_i c_i(\boldsymbol{r},t) \quad (3)$$

$$\frac{\partial c_i(\boldsymbol{r})}{\partial t} + \nabla \cdot \left(\boldsymbol{u}(\boldsymbol{r})c_i(\boldsymbol{r})\right) - \nabla \cdot H_i \nabla\, c_i(\boldsymbol{r}) - \nabla \cdot \frac{\nu_t}{Sc_t}\nabla c_i(\boldsymbol{r}) = \frac{\beta_0}{k_{eff}}\chi_{p,g}\ \sum_{g'=1}^{G}\nu_{g'}\Sigma_{f,g'}\phi_{g'}(\boldsymbol{r}) - \ \lambda_i c_i(\boldsymbol{r}) \quad (4)$$

where

t = time

k_{eff}^{st} = steady-state eigenvalue from a previous steady-state solve

v_g = neutron speed for group g.

For most practical cases, except for prompt critical reactivity insertions, the term $\frac{1}{v_g}\frac{\partial \phi_g(\boldsymbol{r},t)}{\partial t}$ is neglected.

Accurate species tracking in MSRs requires the integration of these neutronics models with thermal-hydraulics and thermomechanics solutions. The distribution of neutron precursors, which affect delayed neutron fractions and reactor kinetics, depends heavily on the flow and temperature fields in the reactor. Any changes in these fields, such as those caused by temperature variations or structural deformations, must be accounted for in the neutronic calculations to ensure accurate predictions of species behavior. This coupling is crucial for predicting the transport and fate of radioactive species, ensuring reactor safety, and optimizing reactor operation.

2.2. Coupling Neutronics and Bateman Solver in Griffin for Species Depletion

In Griffin, the coupling of the neutronics solver to a Bateman solver is needed for computing the isotopic inventory in the reactor core. These isotopes dictate, in turn, the element inventory in the reactor that determines the species formed in this one. The Bateman equations describe the time evolution of isotope concentrations due to nuclear reactions and decay. For a given isotope i, the Bateman equation is as shown in Equation (5):

$$\frac{dN_i(t)}{dt} = -\lambda_i N_i(t) + \sum_j \lambda_{j\to i} N_j(t) + \Sigma_{f,i}\,\phi(t) N_i(t) - \sum_k \Sigma_{ik}\phi(t) N_i(t) \quad (5)$$

where

$N\_i(t)$ = number density of isotope i at time t,

λ_i = decay constant of isotope i,

$\lambda_{j\to i}$ = decay or reaction rate from isotope j to isotope i

$\Sigma_{f,i}$ = fission cross-section for isotope i,

Σ_{ik} = cross-section for the transmutation reaction that depletes isotope i to produce isotope k.

The coupling mechanism implemented for depletion and neutronics goes as follows:

1. Flux Calculation: The neutronics solver computes the neutron flux distribution throughout the reactor core using the temperature and density fields computed by the thermal-hydraulics solver.
2. Reaction Rate Computation: The neutron flux is used to determine reaction rates for each isotope, which are inputs for the Bateman solver.
3. Isotopic Evolution: The Bateman solver uses these reaction rates to solve the Bateman equations, computing the time-dependent isotopic concentrations for the next time step.
4. Feedback Loop: The updated isotopic concentrations alter material properties, such as macroscopic cross sections, which are fed back into the coupled neutronics and thermal-hydraulics solver to recalculate the neutron flux.

This coupling process is iterative and continues over time steps until the desired simulation time is reached. The performed calculations show results at a depletion of 10 $MWd/kgHM$ during the postulated operation of the reactor with ^{235}U. The results obtained for this burnup were obtained by iteratively following the previous process. This coupled approach allows for prediction of the isotopic inventory throughout the reactor's operation, enabling more accurate species tracking.

2.3. Thermal-Hydraulics Modeling for Species Tracking in Molten Salt Reactors

The thermal-hydraulics model in MSRs solves for the conservation of mass, momentum, and energy in the fuel salt. A few particularities of the model added for the MSR solution are the following, which are important for accurately tracking species in MSRs:

- A porous media formulation is used to model the mixing plate and pump structures in the reactor core.
- A weakly compressible formulation is used to account for the thermal heating effects in changing the thermophysical properties.
- A region-dependent mixing-length turbulence model is used to capture turbulent mixing in the reactor pool.

The porous media formulation is crucial for accurately modeling the flow dynamics within complex reactor components such as the mixing plate and pump structures. These components usually have complicated geometries that create significant resistance to flow, leading to pressure drops and localized mixing effects. By treating these regions as porous media, the model can capture the homogenization of flow that occurs as the fluid passes through these structures.

For species tracking, this is important because the distribution and transport of isotopic species are strongly influenced by the flow patterns. The homogenization effects modeled by the porous media formulation help predict how radioactive species are distributed as they pass through the reactor core. Without this accurate representation, there could be significant errors in predicting where species accumulate, how they mix, and where they might plate out or deposit on surfaces within the reactor.

The weakly compressible formulation accounts for the changes in thermophysical properties of the molten salt due to thermal heating. In an MSR, as the reactor operates, the fuel salt heats up, leading to changes in its density, viscosity, and other thermophysical properties. These changes can affect the flow dynamics and, consequently, the transport of species.

For species tracking, accounting for these thermal effects is critical. As the salt heats up and becomes less dense, its ability to carry species through the reactor can change. This affects not only the speed at which species are transported but also their likelihood of depositing on surfaces or precipitating out of the molten salt. Accurate species tracking requires that these thermal effects be modeled so that the distribution of isotopic species under different operating conditions can be predicted with high fidelity.

Turbulence plays a significant role in mixing and species transport within the reactor pool. The region-dependent mixing-length turbulence model captures the variations in turbulence intensity across different regions of the reactor, which is essential for understanding how species are mixed and transported.

In species tracking, turbulence affects the diffusion and dispersion of isotopic species within the molten salt. High turbulence in certain regions can enhance mixing, leading to a more uniform distribution of species, while low turbulence might result in stratification or localized concentrations of species. The region-dependent model ensures that these variations are accurately represented, allowing for precise predictions of species behavior in different parts of the reactor.

The porous media formulation used in Pronghorn, which is NEAMS's coarse-mesh computational fluid dynamics tool, assumes that the liquid fuel and the internal reactor structures occupy the same homogenized space. The fluid volume fraction is referred to as the porosity of the shared volume. In mathematical terms, the porosity of an assembly can be defined as $\gamma = V_f/V_T$, where V_f is the volume of the computational cell occupied by the fluid phase and V_T is the total volume of that cell.

Two-phase flow balance equations for fluid mass, momentum, energy, and solid energy are coupled via momentum and energy exchanges described by correlations. One advantage of this approach is the ability to seamlessly couple porous flow regions to free-flow regions outside of the immediate core regions without changing the modeling paradigm. The porous flow equations for weakly compressible flow are shown in Equation (6) [Narsilio et al. 2009]:

$$\frac{\partial \gamma \rho_m}{\partial t} + \nabla \cdot (\rho_m \boldsymbol{u}_m) = 0, \frac{\partial \gamma \rho_d}{\partial t} + \nabla \cdot (\rho_d \boldsymbol{u}_d) = \Gamma_d$$

$$\frac{\partial \gamma \rho_m}{\partial t} + \nabla \cdot (\gamma^{-1} \rho_m \boldsymbol{u}_m \boldsymbol{u}_m) + \nabla \cdot (\gamma^{-1} \alpha \rho_d \boldsymbol{u}_d \boldsymbol{u}_d) - \nabla \cdot \left[(\mu_m + \rho_m \nu_t) (\nabla u_m + \nabla u_m^T) \right] = -\gamma \nabla p_m + \gamma \rho_m \boldsymbol{g} + \boldsymbol{f}$$

$$\frac{\partial \gamma e_m}{\partial t} + \nabla \cdot (\gamma^{-1} \boldsymbol{u}_m H_m) - \nabla \cdot (\kappa \nabla T) - \nabla \cdot \left(\frac{\nu_t}{Pr_t} \nabla e_m \right) = \dot{q}_l'''$$

(6)

where

α = void fraction

ρ_m = mixture density

$\boldsymbol{u}_m$ = mixture velocity

ρ_d = dispersed gas-phase density

$\boldsymbol{u}_d$ = drift velocity of the dispersed gas phase, which is computed by a closure model

μ_m = mixture molecular viscosity

ν_t = turbulent viscosity, which is computed via a mixing-length model

p_m = mixture pressure

$\boldsymbol{g}$ = acceleration of gravity

$\boldsymbol{f}$ = a volumetric force, which comes due to friction with internal structures or due to momentum sources added at the pumps

e_m = mixture internal energy

H_m = mixture enthalpy

κ = thermal conductivity in the fluid, which is frequently a tensor in the porous media

T = temperature of the liquid-gas mixture

Pr_t = turbulent Prandtl number

$\dot{q}_l'''$ = volumetric heat source deposited directly in the fluid, which during steady-state operation of the MSR, is the power source due to fission and delayed nuclear power.

Each of the intensive mixture variables (e.g., ρ_m) is computed by the mixture average as follows in Equation (7):

$$\rho_m = \alpha\rho_g + (1-\alpha)\rho_l, \tag{7}$$

where

ρ_l = density of the liquid phase.

The mixture velocity is computed by preserving mass flow rates as follows in Equation (8):

$$\boldsymbol{u}_m = \frac{\alpha\rho_g\boldsymbol{u}_d + (1-\alpha)\rho_l\boldsymbol{u}_l}{\rho_m}, \tag{8}$$

where

$\boldsymbol{u}_l$ = velocity of the liquid phase.

Finally, for species tracking, it is important to compute the interface area between the liquid and gas phases. In this work, this interface area ξ_g is determined as follows in Equation (9):

$$\xi_g = \frac{6\alpha}{d_g}, \tag{9}$$

where this model assumes spherical bubbles of diameter d_g. This work takes $d_g \approx 1mm$, which was the average bubble diameter observed for MSRE [Compere et al. 1975].

2.4. Two-Phase Modeling of Species Tracking in Molten Salt Reactors

Species are tracked using an Eulerian approach. In this one, as depicted in Figure 2, the concentration of a species of type i for a state x, named c_i^x, is modeled as a function of space and time. Note that the state x can either be liquid or gas, and i will represent an isotope into our models.

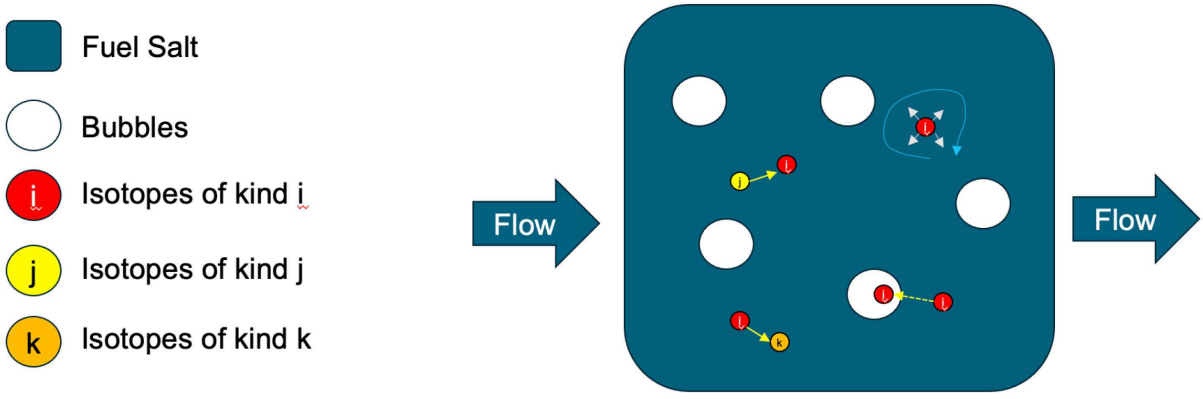

Figure 2. Schematic representation of the model used for species tracking.

The equation for the transport of species in the Eulerian frame reads as follows Equation (10):

$$\frac{\partial c_i^x}{\partial t} + \nabla\cdot\left(\frac{\boldsymbol{u}_m}{\gamma}c_i^x\right) - \nabla\cdot\left[\left(D_{C_i} + \frac{\nu_t}{Sc_t}\right)\nabla c_i^x\right] =$$
$$-\lambda_i c_i^x + \sum_j \lambda_{j\to i} c_i^x + \Sigma_{f,i}\,\phi(t) c_i^x - \sum_k \Sigma_{ik}\phi(t) c_i^x - h^{xy}(c_i^x - c_i^y), \tag{10}$$

where

D_{C_i} = molecular diffusion coefficient

h^{xy} = mass transfer coefficient between the liquid and gas phases.

From left to right, the terms in the species tracking equation are the time derivative, convective derivative, molecular and turbulent diffusion, natural decay, transmutation into the species, production by fission, destruction due to nuclear reactions, and losses due to the transfer to other phases.

2.5. Notes on Developing a General Framework for Species Tracking

In the context of species tracking in MSRs, thermal-hydraulics modeling is integral for predicting the transport and fate of isotopic species within the reactor. The flow field, temperature distribution, and phase changes within the reactor influence how species move and where they accumulate. For example, the deposition of fission products or corrosion products on solid surfaces, the accumulation of radioactive isotopes in cooler regions, and the transport of these species through different reactor regions are all governed by the thermal-hydraulic conditions.

The coupling of neutronics and thermal-hydraulics models is essential for accurate species tracking. The neutronic behavior affects where fission reactions occur and, therefore, where new species are generated. Meanwhile, the thermal-hydraulic behavior determines how these species are transported and where they might precipitate or deposit. For example, temperature gradients can lead to thermophoretic forces that drive species toward certain regions, while flow patterns can enhance or inhibit the mixing of different species.

Additionally, the enthalpy-porosity approach used to model phase changes is particularly important in MSRs where solidification of the fuel salt might occur during transient events. The solidification process can trap species within solid regions, affecting their transport and potentially leading to localized concentrations of radioactivity. Accurately modeling these phase changes and their impact on species distribution is crucial for understanding the overall behavior of radioactive materials in the reactor and for ensuring safe and efficient reactor operation.

The models described here provide the foundation for a comprehensive species tracking framework in MSRs. In the MSRE, this framework allowed researchers to predict the isotopic behavior under various operating conditions and transients. The insights gained from these predictions were critical for ensuring safe and efficient reactor operation. By understanding how species would behave under different scenarios, operators could take proactive measures to manage the reactor's isotopic inventory and maintain its safety.

The integration of these models with advanced computational tools, such as those developed under the NEAMS program, further enhances the accuracy of simulations and species transport analyses. In the context of the MSRE, operators could rely on sophisticated models to predict the movement and accumulation of isotopic species, aiding in the optimization of reactor operations and the design of future MSRs.

The experience gained from the MSRE, combined with these advanced modeling techniques, provides valuable lessons for the design and operation of future MSRs. By building on this foundation, future reactors can achieve even greater efficiency and safety, leveraging the detailed understanding of species tracking developed through experiments like the MSRE.

3. Application to Mixed Liquid-Gas Species Tracking in the Molten Salt Reactor Experiment

3.1. Description of the Molten Salt Reactor Experiment Model

The MSRE, conducted at Oak Ridge National Laboratory between 1965 and 1969, was a project that demonstrated the viability of MSRs [Haubenreich and Engel 1970]. In the context of modeling the MSRE, a 2D axisymmetric approach is applied to capture the essential thermal-hydraulic and neutronic behaviors of the reactor. This model is schematically shown in Figure 3 along with the actual MSRE core that is shown in the left panel of Figure 3. This section details the specific components and assumptions used in the model, illustrating how the circulation of fuel salt, generation of fission power, heat removal, and gas extraction processes are simulated.

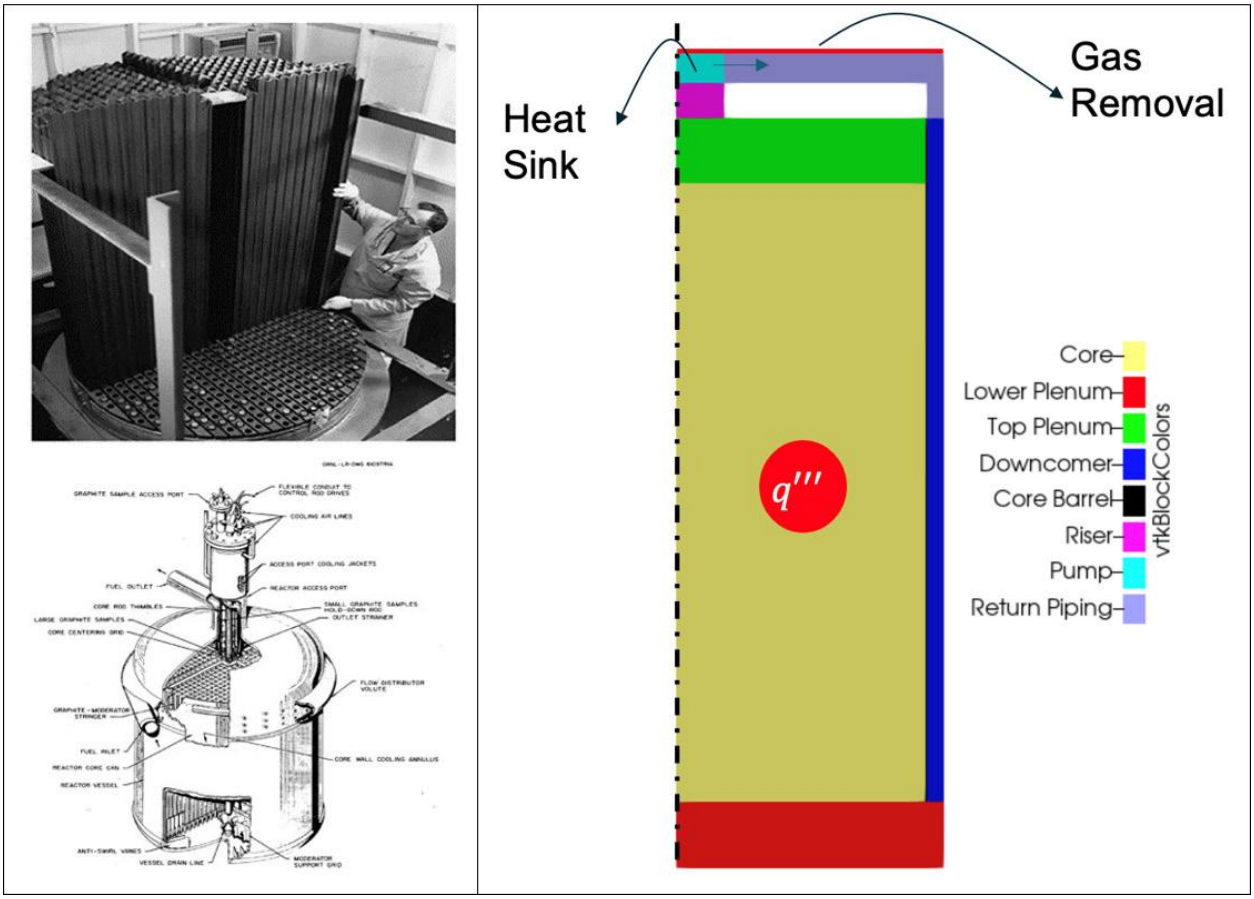

Figure 3. Left: MSRE core (top) and MSRE primary loop cut at the core (bottom). Right: axisymmetric model developed for MSRE [Fratoni et al. 2020].

In the MSRE, the fuel salt—a mixture of uranium tetrafluoride (UF4) dissolved in a molten fluoride salt—circulates through the reactor core, where nuclear fission occurs, then through the heat exchanger. The circulation is driven by a pump located above the riser. In the 2D axisymmetric model, this pump is represented as a momentum source that establishes a flow field within the reactor.

The pump maintains the flow rate of the fuel salt through the core, ensuring that the fission products and other isotopes are transported efficiently. The model simulates the pump's operation by applying a boundary condition that imposes a specified velocity or pressure gradient at the pump location, thus achieving a continuous circulation of the salt. Modeling this circulation is critical for species tracking, as it affects the distribution of fission products, the transport of delayed neutron precursors, and the overall thermal-hydraulic behavior of the reactor.

The MSRE operated with a total thermal power output of 10 MW, generated by nuclear fission reactions within the reactor core. In the 2D axisymmetric model, the core is the primary region of interest, where the neutron flux distribution and corresponding power generation are simulated.

The model calculates the spatial distribution of fission power based on the neutron flux and the fuel composition. The power generation is then coupled with the thermal-hydraulic model to determine the temperature distribution within the core. This temperature distribution influences the fluid dynamics, including buoyancy-driven flows, and the transport of isotopic species.

Accurately modeling the power generation is needed for predicting the behavior of fission products and other species. The high temperatures within the core can lead to increased rates of chemical reactions, potential gas bubble formation, and changes in the solubility of various species. These effects are captured in the model, allowing for a detailed analysis of how the reactor operates under steady-state and transient conditions.

In the MSRE, heat generated in the reactor core is removed by a heat exchanger, where the thermal energy is transferred from the molten salt to a secondary coolant loop. In the 2D axisymmetric model, this heat removal process is simulated by placing a heat sink at the pump location.

The heat sink in the model represents the effect of the heat exchanger, where a portion of the thermal energy is extracted from the fuel salt as it passes through the pump. This boundary condition is implemented by applying a convective heat transfer coefficient or a fixed temperature boundary at the pump location, simulating the removal of heat from the system.

This aspect of the model is critical for maintaining the overall thermal balance of the reactor. By accurately simulating the heat removal process, the model ensures that the temperature distribution within the reactor is realistic, which in turn affects the flow dynamics and species transport. For example, the cooler temperatures near the pump and heat exchanger may lead to the deposition of certain species or the condensation of gases, which must be accurately predicted for effective reactor operation.

One of the unique features of the MSRE was its ability to manage gaseous fission products, such as xenon and krypton, which are produced during the fission process. In the reactor, these gases were extracted from the molten salt to prevent them from affecting reactor performance and safety.

In the 2D axisymmetric model, gas extraction is simulated by imposing a boundary condition at the top of the reactor, where it is assumed that all gases are removed with 100% efficiency. This idealized assumption simplifies the modeling process while capturing the essential behavior of the gas extraction system.

This boundary condition affects the species tracking within the reactor by removing gaseous fission products from the circulating fuel salt. By extracting these gases, the model prevents their accumulation within the core, which could otherwise lead to reactivity changes or challenges in reactor control. The model also considers the impact of gas removal on the overall thermal-hydraulic behavior, as the extraction of gases can influence the density and viscosity of the molten salt, further affecting flow patterns.

3.2. Predicted Void Distribution During Steady-State Operation of the Moten Salt Reactor Experiment

In the MSRE, void formation and distribution affect the reactor's performance and safety and, of particular interest to this work, affect the transport of species between the liquid and gaseous phases. Void refers to gas bubbles within the circulating fuel salt, which can result from fission gas release, temperature changes, and chemical reactions. In this work, void is produced by the direct volatilization of fission gases, which was assumed to be ~2% of the total fission density following estimates from experimental data of MSRE [Compere et al. 1975]. The distribution of voids within the reactor varies as the fuel salt circulates, particularly as it passes through the reactor core and into the upper plenum. The predicted void distribution and interface area concentration during the steady-state operation of the reactor and at a burnup of 10 MWd/kgHM are shown in Figure 4.

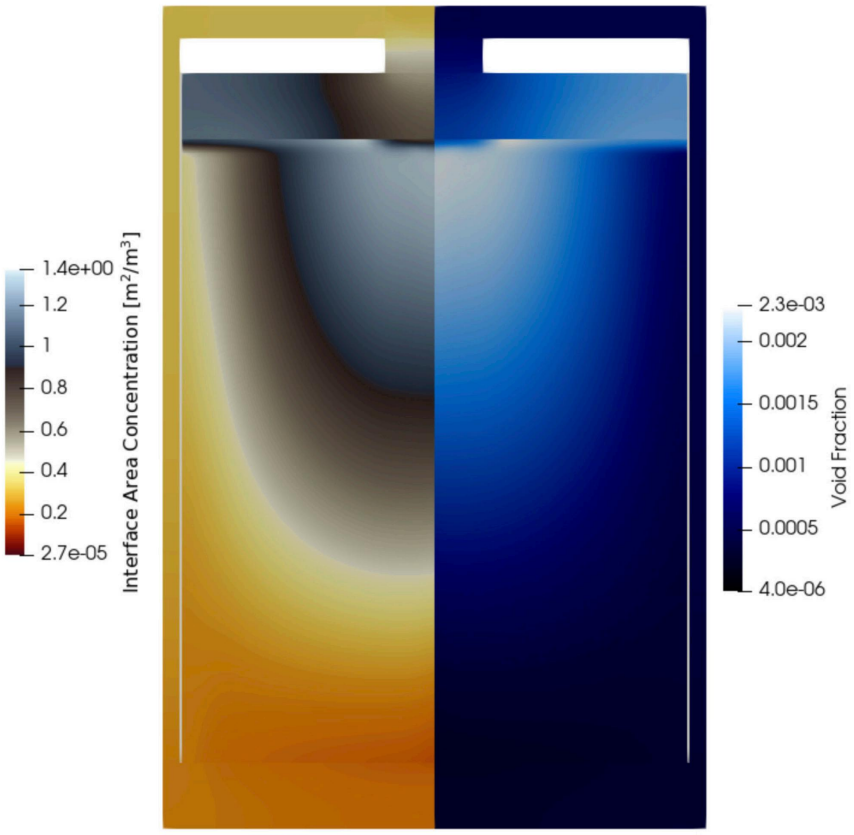

Figure 4. Interface area concentration (left) and void fraction (right) during the steady-state operation of MSRE at 10 MWd/kgHM of burnup. All void is assumed to be produced by the volatilization of fission products (i.e., no gas injection into the system is modeled).

As the fuel salt circulates through the reactor core, voids increase due to the release of gaseous fission products like xenon and krypton. These gases accumulate in the molten salt, forming voids. The rate of void formation is influenced by the neutron flux distribution and temperature within the core, which affect the solubility of gases in the molten salt. Higher temperatures and regions with intense fission activity promote gas release, leading to increased void formation. The molten salt carries these voids into the upper plenum. Upon entering the upper plenum, the flow of molten salt exhibits two distinct behaviors affecting void distribution:

1. Flow Jets to the Riser: In the central region of the upper plenum, the flow jets directly toward the riser, leading to the pump. In this region, voids are efficiently transported upwards and removed at the pump location, where void removal is assumed to be near 100% efficient. This efficient removal maintains a lower void concentration in the central part of the upper plenum.
2. Occluded Flow towards the Outer Radius: As the flow moves toward the outer radius of the upper plenum, it becomes more occluded, trapping voids and leading to a higher concentration of gas bubbles in this region. The occlusion results from the geometry of the plenum and the flow dynamics, causing a decrease in velocity and an increase in bubble retention. Consequently, the outer regions of the upper plenum exhibit higher void concentrations compared to the central riser area.

The void distribution affects the interfacial concentration, which determines the rate of liquid-gas exchange processes. At the top of the reactor core, where molten salt enters the upper plenum, the combination of high temperature and void concentration leads to significant liquid-gas exchange. The interfacial area is large due to the presence of small bubbles, and the high temperatures enhance the rate of gas release from the molten salt. In the partially occluded flow regions towards the outer radius of the upper plenum, the higher void concentration increases the interfacial area, promoting additional gas exchange. However, lower flow velocities and higher void retention in these areas may reduce the efficiency of void removal, as gases mightre-dissolving into the molten salt or form larger bubbles.

3.3. Example of High-Fidelity Tracking of the 91 Depletion Chain in the Molten Salt Reactor Experiment During Steady-State Operation

As an example, an application to demonstrating the high-fidelity tracking of the 91-depletion chain is studied in this section. A representation of this decay chain is shown in Figure 5:

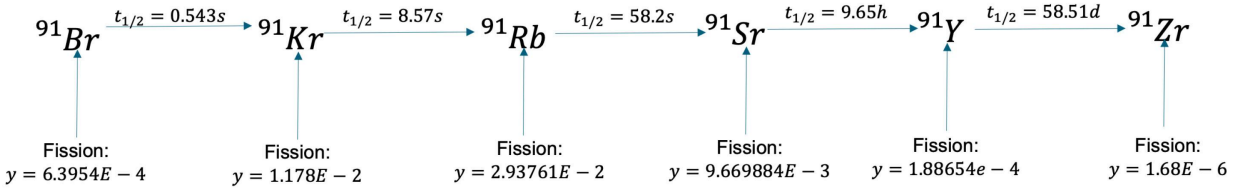

Figure 5. Decay chain representation.

This depletion chain follows this path:

- ^{91}Br (Bromine-91) decays to ^{91}Kr (Krypton-91) ^{91}Kr (Krypton-91) decays to ^{91}Rb (Rubidium-91)
- ^{91}Rb (Rubidium-91) decays to ^{91}Sr (Strontium-91)
- ^{91}Sr (Strontium-91) decays to ^{91}Y (Yttrium-91)
- ^{91}Y (Yttrium-91) decays to ^{91}Zr (Zirconium-91).

All these isotopes are simultaneously produced by fission with the fission yield specified in the Figure 5. While the reactor operates at steady state, many of these isotopes are burned by fission. This section presents detailed results from the simulation of the 91-depletion chain, using the high-fidelity multiphysics model previously described. The model tracks the production, transport, phase change, and eventual off-gassing of these isotopes within the reactor's liquid and gas phases, providing insights into the complex interplay of neutronics, thermal-hydraulics, and species transport.

The results obtained for the high-fidelity species tracking are shown in Figure 6. The behavior of each of the isotopes tracked is described in the following paragraphs.

Bromine-91 is produced primarily as a fission product in the MSRE. Once formed, ^{91}Br remains in solution within the fuel salt. The multiphysics model shows that ^{91}Br does not transition to the gas phase under the operating conditions of the reactor. This behavior can be attributed to the chemical properties of bromine in the molten salt environment, where it remains highly soluble. The lack of gaseous ^{91}Br in the system simplifies the modeling of this isotope, as it does not contribute to the gas-phase dynamics within the reactor. This also implies that the decay of ^{91}Br occurs entirely within the liquid phase of the fuel salt, directly leading to the production of krypton-91 in the same phase.

Krypton-91 is produced through two primary mechanisms: directly from fission and from the beta decay of ^{91}Br in the fuel salt. The behavior of ^{91}Kr as a noble gas is more complex compared to ^{91}Br due to its ability to exist in both liquid and gas phases. Upon production, a portion of ^{91}Kr remains dissolved in the fuel salt, while another portion transitions into the gas phase. The multiphysics model predicts that the partitioning between the liquid and gas phases depends on local temperature, pressure, and the concentration of krypton within the salt. The ^{91}Kr in the gas phase is transported toward the top of the reactor core, where it is eventually removed at the gas extraction point. The model also shows that the transport of ^{91}Kr to the gas phase significantly influences the overall isotopic inventory in the reactor. As ^{91}Kr is removed from the system, the subsequent production of rubidium-91is also affected, reducing the buildup of this isotope in the fuel salt.

Rubidium-91 is produced by both direct fission and the decay of ^{91}Kr in the fuel salt. Additionally, ^{91}Rb is generated by the decay of ^{91}Kr in the gas phase. This dual-source production makes the behavior of ^{91}Rb particularly interesting within the reactor. In the liquid phase, ^{91}Rb remains soluble and contributes to the overall inventory of isotopes within the fuel salt. The multiphysics model indicates that ^{91}Rb does not transition into the gas phase under normal operating conditions, suggesting that it behaves similarly to ^{91}Br in this respect. However, the production of ^{91}Rb in the gas phase, as a result of ^{91}Kr decay, leads to a small but significant accumulation of rubidium in the upper regions of the reactor. The model predicts that this gas-phase ^{91}Rb eventually re-enters the liquid phase as the gas is cooled and processed, contributing back to the liquid-phase isotopic inventory.

Strontium-91 follows a similar production pathway as ^{91}Rb, as it is generated both by direct fission and by the decay of ^{91}Rb in the fuel salt. Like ^{91}Rb, ^{91}Sr remains entirely in the liquid phase within the reactor, with no significant transition to the gas phase observed in the model. The multiphysics model shows that ^{91}Sr is relatively stable within the molten salt, where it contributes to the overall isotopic inventory. Its behavior is important because it acts as a precursor to yttrium-91, another key isotope in the 91-depletion chain. The model's predictions indicate that the concentration of ^{91}Sr in the fuel salt can influence the subsequent production and accumulation of ^{91}Y.

Yttrium-91 is produced in the reactor by direct fission and the decay ^{91}Sr. Unlike earlier isotopes in the chain, ^{91}Y does not participate in any significant liquid-gas exchange processes. The model shows that ^{91}Y remains in the liquid phase throughout its life cycle within the reactor. The stability of ^{91}Y in the liquid phase means that its behavior is largely governed by the local conditions of the fuel salt, such as temperature and flow dynamics. The model indicates that ^{91}Y accumulates in regions of the reactor the fuel salt is more stagnant, leading to localized areas of higher where radioactivity. The absence of gas-phase dynamics for ^{91}Y simplifies its modeling, but the isotope still plays a crucial role in the overall isotopic inventory due to its subsequent decay to zirconium-91.

Zirconium-91 is the final isotope in the 91-depletion chain, produced by the decay of ^{91}Y. Like its immediate precursor, ^{91}Zr remains entirely in the liquid phase, with no significant interactions with the gas phase. The model predicts that ^{91}Zr accumulates over time in the reactor's fuel salt, contributing to the long-term isotopic inventory. Because ^{91}Zr is a stable isotope, it does not decay further, meaning that it represents an end point for the isotopic transformations in the 91-depletion chain. The accumulation of ^{91}Zr in the reactor poses challenges for long-term operation and fuel reprocessing. The high-fidelity model provides insights into where ^{91}Zr is likely to concentrate within the reactor, helping to inform strategies for its management.

The tracking of the 91-depletion chain using the high-fidelity multiphysics model provides a more detailed understanding of the behavior of isotopes, from bromine-91 to zirconium-91, within the MSRE. The model shows how these isotopes are produced, transported, and accumulated, highlighting the need to model exchanges between the liquid and gas phases in the reactor. Even though this is a simple demonstration case, similar models will be performed on future work increasing the number of species that are tracked.

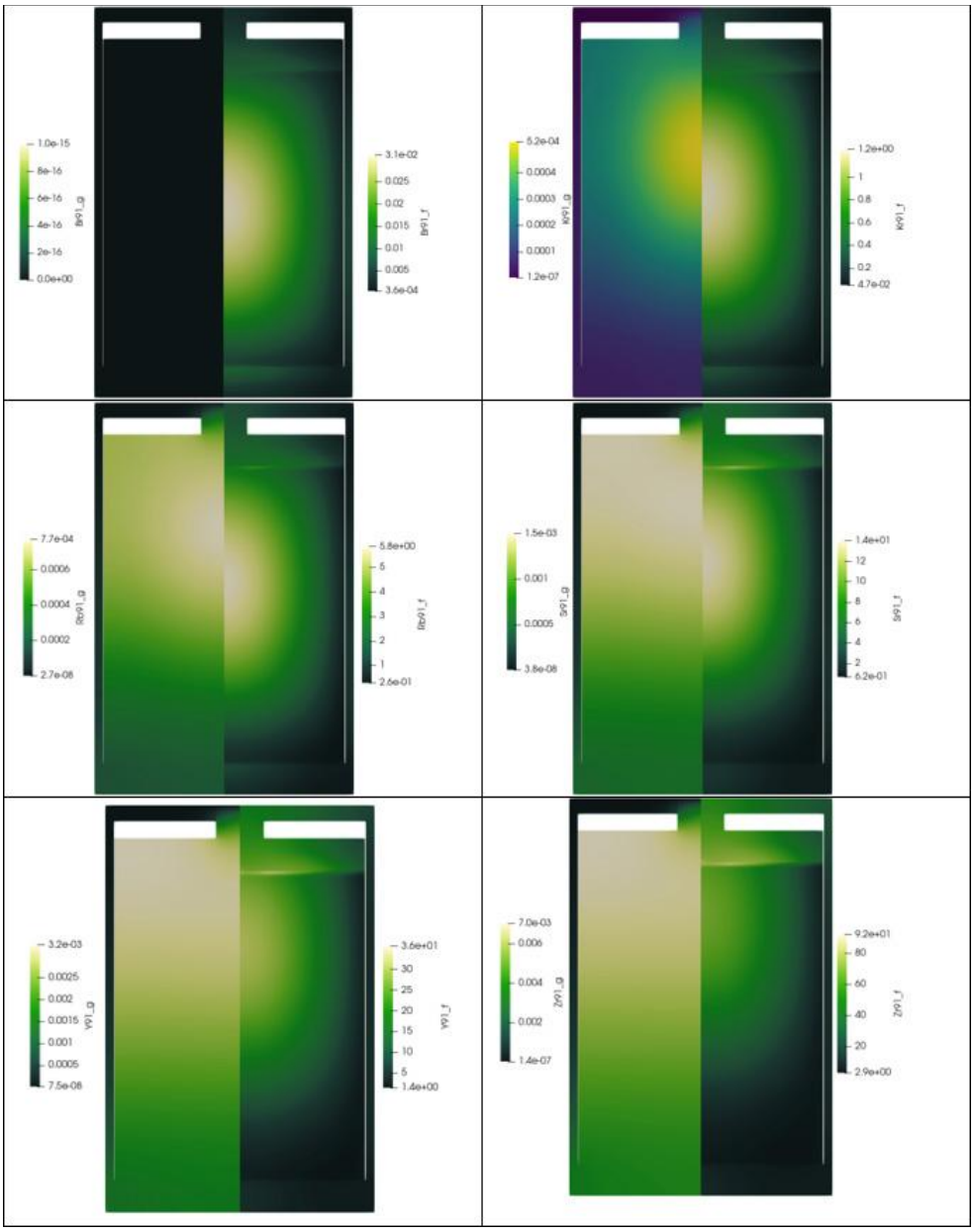

Figure 6. High-fidelity modeling of the distributions for the tracked isotopes in the 91-depletion chain.

The detailed transport performed for these species also have considerable effects in the radiological source term of the MSR. A few observations of each of the isotopes of interest is presented as follows.

Since ^{91}Br does not enter the gas phase, its direct contribution to the gaseous radiological source term is negligible. However, its decay product, ^{91}Kr, partially transitions into the gas phase, where it can be transported and potentially released. The behavior of ^{91}Br thus indirectly influences the source term through its contribution to ^{91}Kr production.

^{91}Kr contributes significantly to the gaseous radiological source term due to its partial presence in the gas phase. The extracted gas phase ^{91}Kr must be accounted for in the reactor's containment and off-gas processing systems. The efficiency of gas extraction at the top of the reactor plays a crucial role in determining the extent of ^{91}Kr's contribution to the source term.

The contribution of ^{91}Rb to the radiological source term is mainly through its presence in the liquid phase, where it contributes to the long-term radioactivity of the reactor. Its presence in the gas phase is transient and less significant for the overall source term, but it highlights the need for accurate tracking of isotopes that may migrate between phases.

^{91}Sr contributes to the radiological source term primarily as a beta-emitting isotope in the liquid phase. Its accumulation over time, particularly in regions of the reactor where flow is more stagnant, could lead to localized increases in radioactivity. Understanding the distribution of ^{91}Sr is essential for assessing the long-term radiological impact of the reactor.

^{91}Y contributes to the radiological source term through its beta decay within the liquid phase. The model shows that while ^{91}Y does not pose significant challenges for gas-phase management, its accumulation in the liquid phase adds to the overall radiological burden of the reactor, particularly in long-term operation scenarios.

While ^{91}Zr is stable and does not contribute to the radiological source term through decay, its accumulation over time increases the heavy metal inventory within the reactor. This accumulation has implications or fuel reprocessing and waste management, as zirconium isotopes may require specific handling during the decommissioning or reprocessing phases. Although ^{91}Zr itself does not contribute to the radiological source term through decay, its presence in the reactor adds to the overall material inventory, which must be managed to maintain reactor safety and efficiency. The model provides insights into the expected distribution of ^{91}Zr, helping to inform strategies for its long-term management.

The model's results emphasize the importance of understanding liquid-gas partitioning, particularly for isotopes like ^{91}Kr, which influence both the liquid and gas phases. Effective species tracking ensures that the reactor operates within safe limits by predicting the movement and accumulation of fission products. The model highlights the critical points within the reactor where isotopes transition between phases or accumulate, providing guidance for monitoring and controlling these processes.

3.4. Example of High-Fidelity Tracking of the 91 Depletion Chain in the Molten Salt Reactor Experiment During a Reactivity Insertion Transient

The methodology developed is applied to evaluate the species evolution in the MSRE during a postulated reactivity insertion transient of 300 pcm. At the onset of the analysis, the reactor is operating at steady-state conditions, characterized by stable temperature and void distributions within the molten salt. Upon the sudden introduction of 300 pcm reactivity, the reactor experiences a rapid power increase, resulting in significant thermal feedback effects. The immediate consequence of this power burst is a sharp rise in the temperature of the reactor core. The evolution of the reactor physics fields is shown in Figure 7.

This temperature increase has a dual effect on reactor behavior. First, it enhances the solubility of gaseous fission products in the molten salt, initially retaining more fission gases within the liquid phase. However, as the temperature continues to rise, the molten salt approaches saturation, leading to an overproduction of voids within the reactor. These voids, primarily composed of gaseous fission products, form rapidly in the first few seconds of the transient.

The formation of voids within the core introduces a significant negative reactivity coefficient. This negative feedback mechanism is a critical aspect of the reactor's inherent safety features, as it counteracts the initial reactivity insertion by reducing the neutron population in the core, thereby lowering the reactor power. The interplay between the temperature rise and void formation is central to the reactor's response during the transient. As the negative reactivity takes effect, it slows down the power excursion, eventually stabilizing the reactor at a new, lower power level.

Despite the reduction in reactor power, the transient leaves a significant amount of void trapped within the reactor system. This trapped void, primarily located in regions of reduced flow such as the upper plenum and along the outer edges of the core, poses a challenge for reactor stability. The voids facilitate the transport of gaseous fission products toward the upper regions of the reactor, where they are ultimately evacuated into the off-gas system.

The evacuation of these gases during the transient has several implications. It temporarily increases the radiological source term in the off-gas system, necessitating careful monitoring and management to prevent any release into the environment. Additionally, the presence of voids and the associated reduction in liquid density can alter local neutron flux distributions, potentially impacting the long-term behavior of the reactor if not properly managed.

The transient behavior and the spatial-temporal evolution of key reactor fields, such as temperature, void fraction, and fission product distribution, are illustrated in Figure 7. These results provide a detailed understanding of how the reactor responds to sudden reactivity changes and highlight the importance of accurately modeling species transport and thermal-hydraulic feedback mechanisms to ensure reactor safety during transient events. The analysis underscores the need for robust off-gas handling systems and effective reactor control strategies to manage the consequences of such transients.

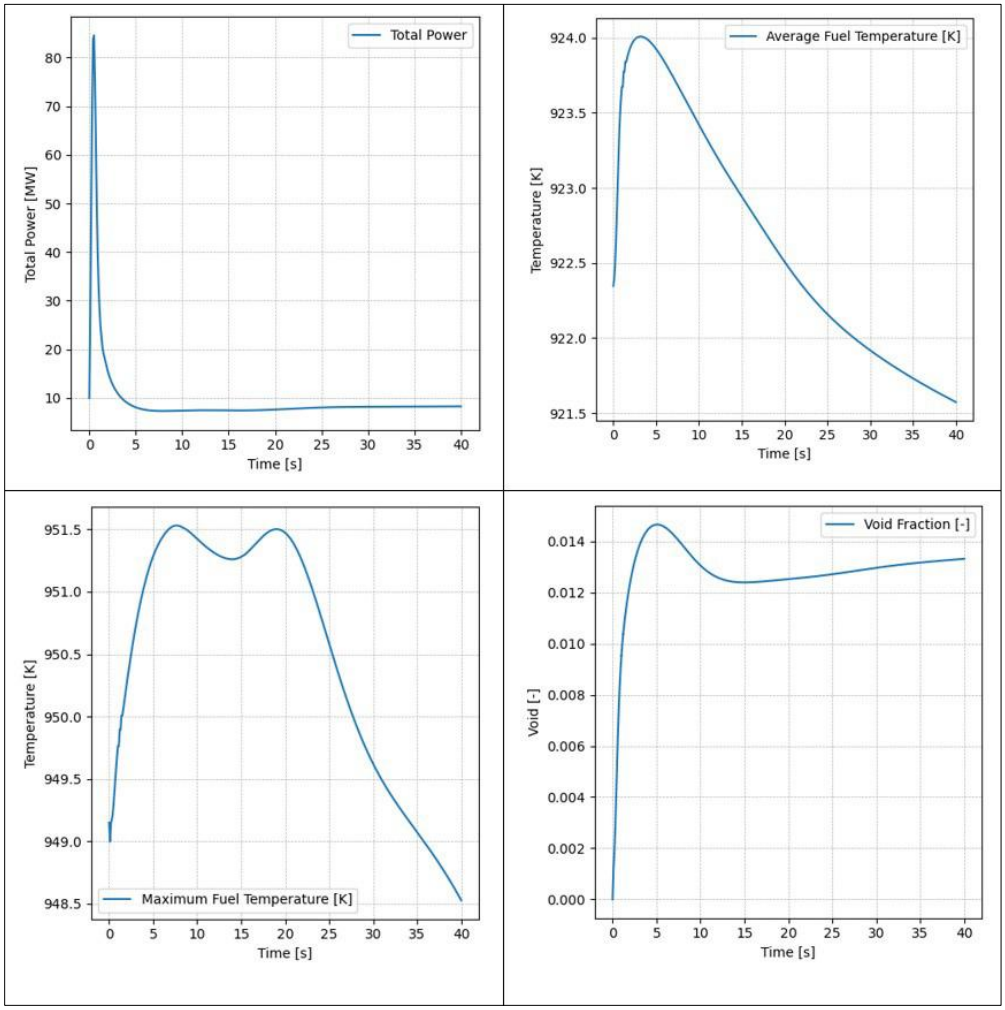

Figure 7. Evolution of reactor physics fields during reactivity insertion transient in MSRE. Top-left: reactor power. Top-right: average fuel temperature. Bottom-left: Maximum fuel temperature. Bottom-right: average void fraction.

The evolution of the isotopes in the 91-depletion chain during the reactivity insertion transient is shown in Figure 8. The results indicate that the relative concentration of isotopes remains similar to the steady-state distribution, with notable shifts in timing due to the decay processes from bromine to zirconium. Specifically, the decay chain exhibits a time lag as the isotopes transition from bromine-91 (^{91}Br) through subsequent intermediates, eventually reaching zirconium-91 (^{91}Zr). This lag is influenced by the varying half-lives of the isotopes involved, as well as the transient conditions imposed by the reactivity insertion.

The increase in gas-phase concentrations during the transient is primarily driven by the overproduction of voids within the reactor core. As the reactivity insertion causes a rapid rise in temperature, voids are generated, promoting the transfer of isotopes from the dissolved liquid phase into the gas phase. This phase transition is particularly evident for isotopes like krypton-91 (^{91}Kr), which are more prone to entering the gas phase under high-temperature conditions.

Initially, the gas-phase concentrations of these isotopes spike due to the sudden influx of voids, which act as carriers, transporting the gaseous fission products upward within the reactor. This increase is a direct consequence of the transient conditions and the resulting shift in the reactor's thermal-hydraulic equilibrium.

Over time, as the voids begin to be removed from the system, the gas-phase concentrations stabilize. This stabilization occurs as the reactor's cooling systems and off-gas management processes gradually return the system to its initial equilibrium state. The isotopes that had entered the gas phase are either evacuated through the off-gas system or re-dissolved into the molten salt as the temperature decreases and voids collapse. Eventually, the concentrations of these isotopes in both the liquid and gas phases return to the levels observed during steady-state operation, reflecting the reactor's ability to self-regulate and achieve a new balance post-transient.

The behavior of the 91-depletion chain during this transient shows the dynamic interactions between isotope production, decay, and phase changes within the reactor. It underscores the importance of accurately modeling both the neutron kinetics and thermal-hydraulic conditions to predict isotope behavior during such events. The eventual return to equilibrium suggests that the reactor's design and control systems are effective in managing the challenges posed by reactivity insertions, though the transient phase represents a period of increased radiological activity that must be carefully managed. The observed time lag in isotope decay also suggests potential areas for optimization in reactor operation, particularly in enhancing the efficiency of off-gas removal systems to better handle the temporary increase in fission product gases.

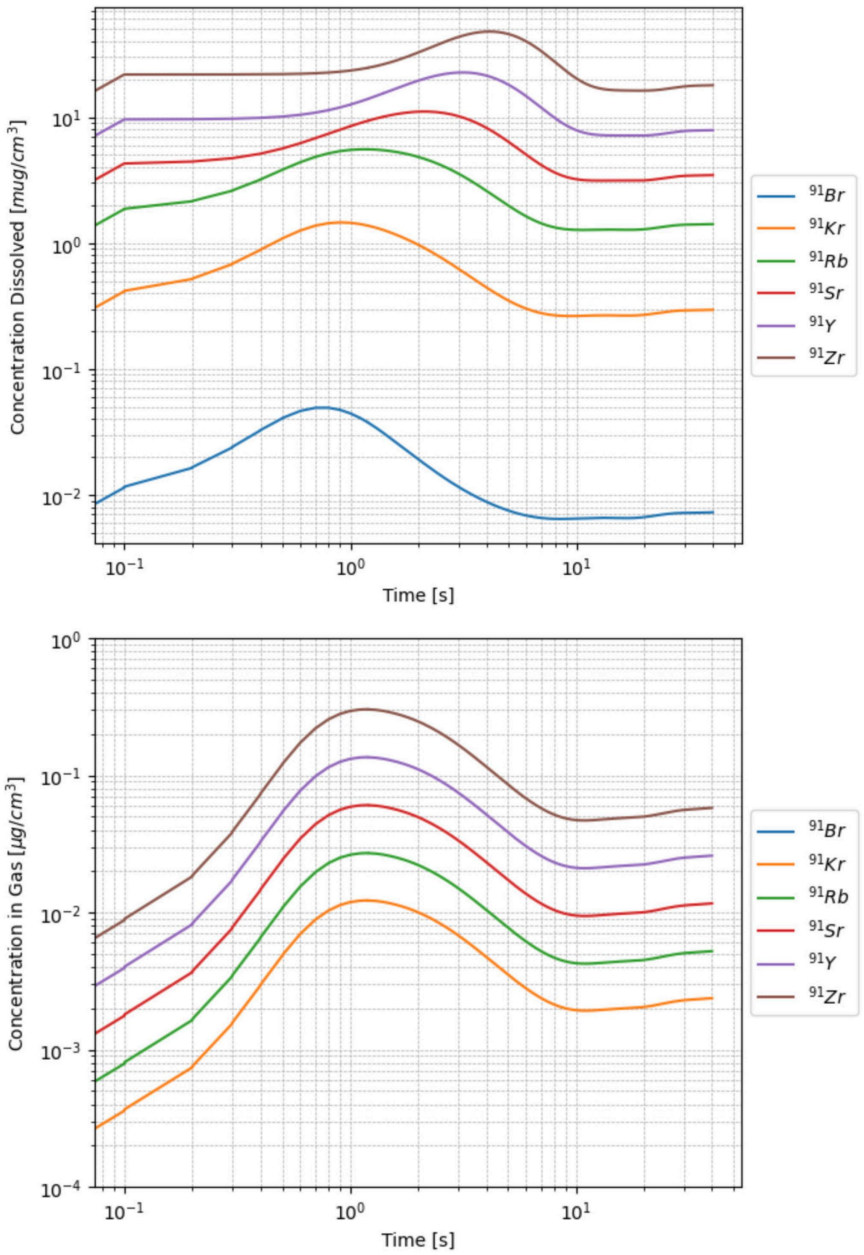

Figure 8. Evolution of the average concentration of the isotopes of the 91-depletion chain in the MSRE during the reactivity insertion transient. Top: concentration of isotopes dissolved in the fuel salt. Bottom: concentration of isotopes in the gas phase.

The accumulated mass of isotopes in the 91-depletion chain within the off-gas system during the reactivity insertion transient is presented in Figure 9. This analysis focuses solely on the isotopic contributions resulting from the transient event, excluding the background distribution established during steady-state operation. The dissolution of species and their transport through the gas system are the two main factors influencing the isotopic distribution observed in the off-gas during this transient.

During the transient, the behavior of the tracked elements in the molten salt plays a critical role in determining which isotopes contribute to the off-gas system. Although zirconium-91 (^{91}Zr) shows the highest concentration within the molten salt during the transient, its contribution to the off-gas system is relatively low. This is primarily due to zirconium's good solubility in the molten salt, which prevents it from readily entering the off-gas system phase. The high solubility means that even as zirconium accumulates in the molten salt, it remains dissolved and does not significantly transition into the gas phase, limiting its presence in the off-gas system.

In contrast, yttrium-91 (^{91}Y), despite being produced in smaller quantities than zirconium, contributes more significantly to the off-gas system. Yttrium's solubility in the molten salt is lower than that of zirconium, making it more prone to transitioning into the gas phase when voids form during the transient. As the molten salt heats up and voids are generated, yttrium is more likely to be swept into the gas phase, where it is carried to the off-gas system. This results in yttrium being a primary contributor to the radiological source term in the off-gas during the transient, despite its lower overall concentration in the molten salt.

The accumulation of rubidium-91 (^{91}Rb) and krypton-91 (^{91}Kr) in the off-gas system also follows a similar pattern. Both isotopes exhibit moderate solubility in the molten salt, leading to their partial transition into the gas phase. Rubidium, while more soluble than krypton, still enters the gas phase in sufficient quantities due to the high temperature and the dynamic conditions of the transient. Krypton, a noble gas, is particularly prone to existing in the gas phase, making it a consistent presence in the off-gas system. The model predicts that the masses of zirconium, rubidium, and krypton in the off-gas system are similar, reflecting their combined behaviors in response to the transient conditions.

Bromine-91 (^{91}Br), conversely, contributes the least to the off-gas system. Bromine remains highly soluble in the molten salt throughout the transient, and its transition into the gas phase is minimal. This limited transition is consistent with the behavior observed during steady-state operation, where bromine remains predominantly in the liquid phase. Consequently, bromine's presence in the off-gas system is significantly lower than that of the other isotopes in the 91-depletion chain.

The results highlight the importance of understanding the solubility and phase behavior of different isotopes in MSRs. The ability of certain elements to transition between liquid and gas phases directly impacts their contribution to the radiological source term in the off-gas system. For instance, while zirconium accumulates within the molten salt, its limited presence in the off-gas system reduces its impact on the radiological source term during the transient. Conversely, elements, such as yttrium, with lower solubility, pose a greater challenge for off-gas management due to their higher volatility under transient conditions.

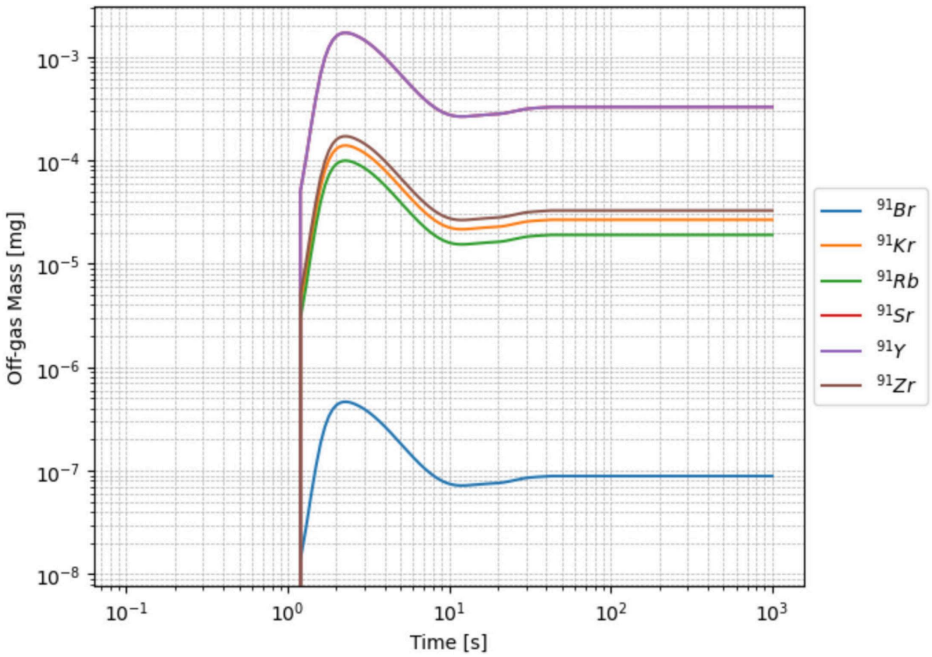

Figure 9. Accumulation of the mass of 91-depletion chain isotopes in the off-gas system during a reactivity insertion transient for MSRE.

The source term in the off-gas system due to the 91-depletion chain during the reactivity insertion transient is shown in Figure 10. Initially, the source term increases as short-lived isotopes are entrained into the off-gas system, driven by the rapid formation of voids and their subsequent transport. As the transient progresses, the source term stabilizes and approaches an equilibrium value, dominated by the decay of longer-lived isotopes that persist in the system.

This behavior highlights the importance of employing higher-fidelity dynamic simulations to accurately compute the off-gas source term in MSRs. The transient nature of isotope production, phase transitions, and decay processes requires detailed modeling to capture the temporal changes in the off-gas system accurately. Without such simulations, the complexities of isotope behavior during transients could lead to underestimation or overestimation of the radiological source term, impacting reactor safety and off-gas management strategies.

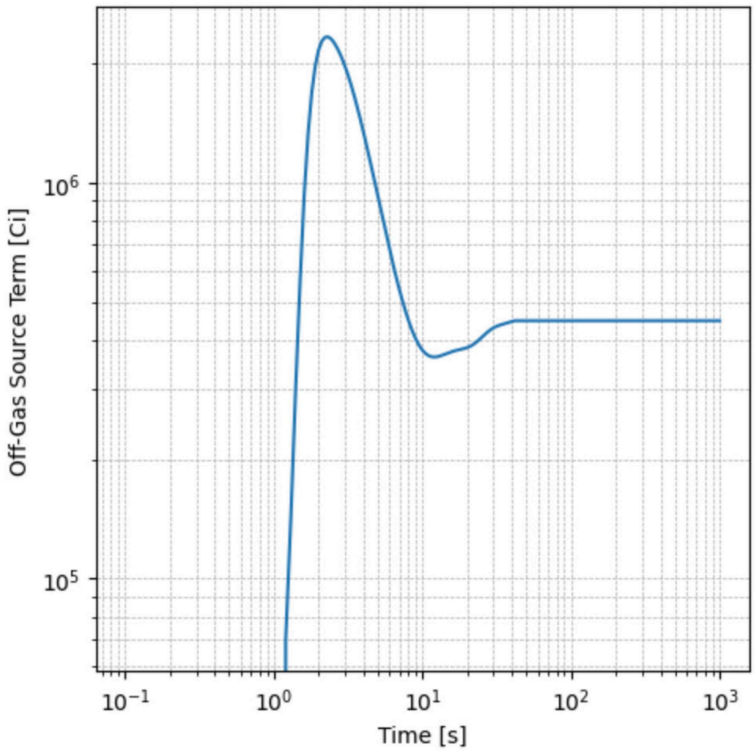

Figure 10. Computed source term in the off-gas system from the 91-depletion chain during a reactivity insertion transient for MSRE.

4. Conclusions, Implications, and Future Work

This work demonstrates a high-fidelity coupling framework using the toolkit developed under the NEAMS program for two-phase species tracking in MSRs. Through the development and application of these multiphysics models, this study has provided insights into the behavior of isotopic species, particularly those in the 91-depletion chain, under both steady-state and transient conditions in the MSRE. This work also shows how multiphysics models may be needed for accurate tracking of species in MSRs.

The main conclusions of this work are the following:

- The tracking of isotopes within the 91-depletion chain showed a considerable interaction between phase transitions, chemical solubility, and reactor thermal-hydraulics. The results underscore that isotopes, such as bromine-91 (^{91}Br), remain largely in the liquid phase, while others like krypton-91 (^{91}Kr) and yttrium-91 (^{91}Y) can transition to the gas phase, significantly influencing the reactor's radiological source term. Additionally, due to the coupled depletion chain, significant content of the isotopes determining the source term in the off-gas system are gas-borne isotopes that appear in the gaseous phase due to the decay of a gaseous precursor. The models also highlighted the importance of understanding isotope-specific behaviors such as the solubility of zirconium-91 (^{91}Zr) in the molten salt, which affects its accumulation and presence in the off-gas system due to the gas-born transport mechanism previously mentioned.
- This work has also shown a significant effect of reactor transients on species tracking. During reactivity insertion transients, the rapid formation of voids and the resulting phase transitions significantly altered the distribution of isotopes in the reactor. The enlarged liquid-gas interface that is produced by the increase of void, results in a significant transfer of previously dissolved isotopes into the gas phase. The observed time lag in the decay chain, especially the delayed transfer of isotopes to the gas phase, pointed to the importance of dynamic simulations in capturing these effects accurately.
- The study also provided a detailed assessment of the source term in the off-gas system, showing that while short-lived isotopes dominate the initial response to transients, longer-lived isotopes eventually dictate the equilibrium state. The multiphysics interaction between isotope solubility, gas-phase transitions, and off-gas management highlights the need for accurate modeling to ensure reactor safety.

In terms of MSR design, operation, and analysis, the following key points can be derived from this work:

- Isotopic distributions in MSRs show a non-homogeneous distribution in the reactor core. This distribution ultimately leads to non-constant transfers into the gaseous phase and non-uniform depletion of isotopes. Hence, for source-term modeling, higher accuracy multiphysics models are needed. These models can either be used to perform high-fidelity analyses of species tracking when the available computational resources are substantial or to train surrogate models that allow for faster source term modeling.
- The multiphysics coupling that ultimately governs species transport, involving coupled neutronics, thermal-hydraulics, depletion, and thermochemistry, complicates a-priori simplifications when tracking species. This work does not disregard simplified analyses; however, due to the results obtained, we recommend that simplifications in species tracking are done a-posteriori (i.e., once a multiphysics model is available to test the validity and impact of these simplifications).

Finally, future work that will enhance the results in this work and further verify its validity would be the following:

- Expand the scope of species tracking to include a broader range of isotopes and chemical species, particularly those relevant to different MSR fuel cycles. This will provide a more comprehensive understanding of the behavior of all critical isotopes within the reactor environment.
- The methodologies developed in this study can be adapted and integrated into the design and operation of next-generation MSRs and other advanced reactor systems. Applying these techniques to new reactor designs will help validate their safety and performance under a wider range of operating conditions.
- Continued development of high-fidelity dynamic models will be essential for capturing the transient behavior of isotopes during more complex operational scenarios, including emergency shutdowns, power ramps, and other off-normal conditions. These models will improve the accuracy of predictions and enhance the reliability of reactor safety systems.
- Further experimental studies are needed to validate the model predictions, particularly concerning the solubility, phase transitions, and transport behaviors of specific isotopes in molten salts. Collaboration with experimental programs can provide the data necessary to refine and calibrate the models, ensuring their accuracy and applicability to real-world reactor operations.

5. REFERENCES

Andrews, H. B., et al. 2021. "Review of Molten Salt Reactor Off-Gas Management Considerations." *Nuclear Engineering and Design* 385: 111529. https://doi.org/10.1016/j.nucengdes.2021.111529.

Aufiero, M., et al. 2014. "Calculating the Effective Delayed Neutron Fraction in the Molten Salt Fast Reactor: Analytical, Deterministic and Monte Carlo Approaches." *Annals of Nuclear Energy* 65: 78–90. https://doi.org/10.1016/j.anucene.2013.10.015.

Compere, E. L., et al. 1975. "Fission Product Behavior in the Molten Salt Reactor Experiment." ORNL-4865. Oak Ridge National Laboratory, Oak Ridge, TN.

Fratoni, M., et al. 2020. "Molten Salt Reactor Experiment Benchmark Evaluation." DOE-UCB-8542. Univ. of California, Berkeley, CA; Oak Ridge National Laboratory, Oak Ridge, TN.

Gill, D. F., and Y. Y. Azmy. 2011. "Newton's Method for Solving K-Eigenvalue Problems in Neutron Diffusion Theory." *Nuclear Science and Engineering* 167(2): 141–153. https://doi.org/10.13182/NSE09-98.

Haubenreich, P. N., and J. R. Engel. 1970. "Experience with the Molten-Salt Reactor Experiment." *Nuclear Applications and Technology* 8(2): 118–136. https://doi.org/10.13182/NT8-2-118.

Ho, M. K. M., G. H. Yeoh, and G. Braoudakis. 2013. "Molten Salt Reactors." In *Materials and Processes for Energy: Communicating Current Research and Technological Developments*, edited by A. Méndez-Vilas, 761–768. Formatex.

Kovacic, Donald N., Andrew Worrall, Louise G. Worrall, George Flanagan, David Holcomb, Robert Bari, Lap Cheng, et al. 2018. "Safeguards Challenges for Molten Salt Reactors." In proceedings of the INMM Annual Meeting, Baltimore, MD, July 22–26.

Krepel, J., U. Rohde, U. Grundmann, and F. P. Weiss. 2008. "Dynamics of Molten Salt Reactors." *Nuclear Technology,* 164(1): 34–44. https://doi.org/10.13182/NT08-A4006.

Mcfarlane, J, et al. 2020. “Molten Salt Reactor Engineering Study for Off-Gas Management.” ORNL/TM-2020/1602. Oak Ridge National Laboratory, Oak Ridge, TN. https://doi.org/10.2172/1649021.

Narsilio, G. A., et al. 2009. “Upscaling of Navier–Stokes Equations in Porous Media: Theoretical, Numerical and Experimental Approach.” *Computers and Geotechnics* 36(7): 1200–1206. https://doi.org/10.1016/j.compgeo.2009.05.006.

Sandhi, K. K. 2022. “Coatings for Alloys Used in Molten Salt Nuclear Reactor.” PhD diss., University of Saskatchewan, Saskatoon, Saskatchewan, Canada.

Sridharan, K., and T. R. Allen. 2013. “Corrosion in Molten Salts.” *Molten Salts Chemistry* 241–267. https://doi.org/10.1016/B978-0-12-398538-5.00012-3.

Walker, S. A., M. E. Tano Retamales, A. Abou Jaoude. 2023. “Application of NEAMS Multiphysics Framework for Species Tracking in Molten Salt Reactors.” INL/RPT-23-74376, Rev 0. Idaho National Laboratory, Idaho Falls, ID.

Worrall, A., et al. 2018. “Molten Salt Reactors and Associated Safeguards Challenges and Opportunities.” IAEA-CN-267, International Atomic Energy Agency, Vienna, Austria. https://www.osti.gov/servlets/purl/1630525.

Zhang, J., et al. 2018. “Redox Potential Control in Molten Salt Systems for Corrosion Mitigation.” *Corrosion Science* 144: 44–53. https://doi.org/10.1016/j.corsci.2018.08.035.